

The sodium channel $\beta 1$ subunit mediates outgrowth of neurite-like processes on breast cancer cells and promotes tumour growth and metastasis

Michaela Nelson¹, Rebecca Millican-Slater², Lorna C. Forrest¹ and William J. Brackenbury¹

¹Department of Biology, University of York, Heslington, York, YO10 5DD, United Kingdom

²Department of Histopathology, St James's University Hospital, Leeds, LS9 7TF, United Kingdom

Voltage-gated Na⁺ channels (VGSCs) are heteromeric proteins composed of pore-forming α subunits and smaller β subunits. The β subunits are multifunctional channel modulators and are members of the immunoglobulin superfamily of cell adhesion molecules (CAMs). $\beta 1$, encoded by *SCN1B*, is best characterized in the central nervous system (CNS), where it plays a critical role in regulating electrical excitability, neurite outgrowth and migration during development. $\beta 1$ is also expressed in breast cancer (BCa) cell lines, where it regulates adhesion and migration *in vitro*. In the present study, we found that *SCN1B* mRNA/ $\beta 1$ protein were up-regulated in BCa specimens, compared with normal breast tissue. $\beta 1$ upregulation substantially increased tumour growth and metastasis in a xenograft model of BCa. $\beta 1$ over-expression also increased vascularization and reduced apoptosis in the primary tumours, and $\beta 1$ over-expressing tumour cells had an elongate morphology. *In vitro*, $\beta 1$ potentiated outgrowth of processes from BCa cells co-cultured with fibroblasts, *via trans*-homophilic adhesion. $\beta 1$ -mediated process outgrowth in BCa cells required the presence and activity of fyn kinase, and Na⁺ current, thus replicating the mechanism by which $\beta 1$ regulates neurite outgrowth in CNS neurons. We conclude that when present in breast tumours, $\beta 1$ enhances pathological growth and cellular dissemination. This study is the first demonstration of a functional role for $\beta 1$ in tumour growth and metastasis *in vivo*. We propose that $\beta 1$ warrants further study as a potential biomarker and targeting $\beta 1$ -mediated adhesion interactions may have value as a novel anti-cancer therapy.

Although the death rate from breast cancer (BCa) is falling in many countries, it is still the leading cause of cancer-related deaths in women, due to metastasis.^{1,2} To metastasize,

tumour cells undergo a complex sequence of events, including adhesion/detachment, migration, and invasion. Given that treatment options for metastatic BCa are mainly restricted to palliation, it is necessary to better understand the mechanism(s) involved in order to identify new targets and develop new therapies.³

Key words: adhesion, breast cancer, fyn kinase, metastasis, voltage-gated Na⁺ channel

Abbreviations: BCa: breast cancer; CAM: cell adhesion molecule; CHL: Chinese hamster lung; CNS: central nervous system; DMEM: Dulbecco's modified eagle medium; ER: estrogen receptor α ; FAK: focal adhesion kinase; GFP: green fluorescent protein; HNA: human nuclear antigen; ICA: intensity correlation analysis; ICC: immunocytochemistry; ICQ: intensity correlation quotient; IHC: immunohistochemistry; VGSC: voltage-gated Na⁺ channel
Additional Supporting Information may be found in the online version of this article.

This is an open access article under the terms of the Creative Commons Attribution License, which permits use, distribution and reproduction in any medium, provided the original work is properly cited.

Grant sponsor: Medical Research Council; **Grant number:** G1000508

DOI: 10.1002/ijc.28890

History: Received 6 Nov 2013; Accepted 3 Apr 2014; Online 12 Apr 2014

Correspondence to: Dr. William J. Brackenbury, Department of Biology, University of York, Wentworth Way, Heslington, York YO10 5DD, UK, Tel: +44-1904-328284, Fax: +44-1904-328505, E-mail: william.brackenbury@york.ac.uk

Voltage-gated Na⁺ channels (VGSCs) contain one pore-forming α subunit with smaller β subunits.⁴ There are nine α subunits, Na_v1.1-Na_v1.9, and four β subunits, $\beta 1$ - $\beta 4$. The β subunits are members of the immunoglobulin superfamily of cell adhesion molecules (CAMs). They modulate channel gating, and can function as CAMs both in the presence and absence of α subunits.⁵ They are substrates for secretase cleavage, releasing soluble intracellular domains that may regulate gene expression.⁶ The $\beta 1$ subunit (gene: *SCN1B*) participates in *trans*-homophilic adhesion, resulting in cellular aggregation and cytoskeleton recruitment.^{7,8} $\beta 1$ also interacts heterophilically with other CAMs, including $\beta 2$, contactin, neurofascins, NrCAM, N-cadherin⁹⁻¹² and the extracellular matrix protein, tenascin-R.¹³ $\beta 1$ mediates neurite outgrowth by a *trans*-homophilic adhesion mechanism that requires fyn kinase, contactin and γ -secretase activity.^{5,14,15} $\beta 1$ plays a critical role during central nervous system (CNS) development, regulating electrical excitability, proliferation, fasciculation, pathfinding and migration.¹⁵⁻¹⁷

VGSCs are widely expressed in cancers, and contribute to cellular behaviours associated with metastasis.^{18,19} In BCa,

What's new?

Voltage-gated sodium channels are best known to regulate electrical excitability and neuronal migration, but recently their $\beta 1$ subunits were found expressed in breast cancer cell lines where they regulate cellular adhesion and migration. Here, the authors demonstrate that $\beta 1$ subunits are expressed in clinical breast cancer specimens. In coculture experiments, $\beta 1$ enhanced outgrowth of neurite-like processes on cancer cells and in *in vivo* models, accelerated tumor growth and metastasis. These data underscore the new role of voltage-gated sodium channel $\beta 1$ subunits as potential biomarkers and therapeutic targets in breast cancer.

the predominant α subunit, $\text{Na}_v1.5$ (gene: *SCN5A*), is expressed in MDA-MB-231 cells, where Na^+ current potentiates invasion by enhancing cysteine cathepsin activity.^{20–22} *SCN5A* is up-regulated in tumours, associating with recurrence, metastasis and reduced survival.^{20,23} $\beta 1$ is the predominant β subunit in MCF-7 cells, where it enhances cell-substrate adhesion, but slows transwell migration.²⁴ Over-expression of $\beta 1$ in MDA-MB-231 cells increases cell-cell adhesion and Na^+ current.²⁴ Both α and $\beta 1$ subunits are expressed in lamellipodia of MCF-7 and MDA-MB-231 cells, suggesting that their expression and function are not mutually exclusive.²³ Thus, VGSC α and β subunits appear to play complex, dynamic roles in metastatic BCa cells. However, the functional significance of $\beta 1$ -dependent adhesion, and its contribution to tumour growth and metastasis, are unknown.

Our aim here was to study the involvement of $\beta 1$ in BCa progression *in vivo*. We show that *SCN1B* mRNA/ $\beta 1$ protein are upregulated in BCa specimens, compared with normal breast tissue. Up-regulation of $\beta 1$ potentiates tumour growth and metastasis *in vivo*. In addition, $\beta 1$ increases process outgrowth on BCa cells *via* a *trans*-homophilic adhesion mechanism that requires fyn kinase and Na^+ current. We propose that $\beta 1$ enhances metastatic behaviour of BCa cells by recapitulating mechanism(s) that are critical for neuronal migration during CNS development. These findings suggest that $\beta 1$ warrants further study as a potential biomarker/therapeutic target.

Methods***In silico* analysis**

SCN1B expression in microarrays was studied using OncoPrint.²⁵ Meta-analysis of correlations between *SCN1B* expression and histoclinical characteristics across multiple datasets was as described.²⁶ Datasets, patients, specimen characteristics and assay methods are detailed/referenced at www.oncoPrint.org.

Cell culture

Molecular identity of all BCa cell lines was confirmed by short tandem repeat analysis. All cell lines were grown in Dulbecco's modified eagle medium (DMEM) supplemented with 5% fetal bovine serum and 4 mM L-glutamine.²³ BT474 and SKBR3 cells were a gift from J. Rae, University of Michigan. MCF-7 and MDA-MB-231 cells were a gift from

M. Djamgoz, Imperial College London. "Control" MDA-MB-231 cells stably expressing enhanced green fluorescent protein (GFP) or MDA-MB-231 cells over-expressing $\beta 1$ -GFP C-terminal fusion²⁴ (hereafter called "MDA-MB-231- $\beta 1$ " cells) were maintained in medium containing selective antibiotics. MCF-10A cells were a gift from N. Maitland, University of York. R1610 Chinese hamster lung (CHL) fibroblasts and CHL fibroblasts stably expressing $\beta 1$ were gifts from L. Isom, University of Michigan. MDA-MB-231-GFP and MDA-MB-231 $\beta 1$ -GFP cells were stably transduced with recombinant lentivirus for firefly luciferase (AMS Biotechnology). For experiments using estrogen, MCF-7 cells were maintained in phenol red-free DMEM supplemented with 5% charcoal-stripped fetal bovine serum and 4 mM L-glutamine. Cells were confirmed as mycoplasma-free using the DAPI method.

Pharmacology

Tetrodotoxin (TTX) was diluted in culture medium to 30 μM . Staurosporine, PP2, estradiol and fulvestrant were prepared as stocks in DMSO and then diluted in culture medium to 10 nM–30 μM . In assays that exceeded 24 h, treatments were replaced daily. The effect of TTX on invasion was determined using Matrigel assays.²³ The effect of staurosporine on apoptosis was determined using DeadEnd fluorometric TUNEL assays (Promega). The effect of PP2 on cell viability and proliferation was determined using trypan blue and MTT assays.²³

RNA isolation and RT-qPCR

RNA extraction and cDNA synthesis were as described.²⁷ QPCR was carried out using triplicate 12- μl reactions containing 20ng cDNA. Amplification conditions were: 95°C for 30 s followed by 35 cycles of 95°C for 5 s and 60°C for 10 s on a Bio-Rad thermal cycler. Relative gene expression was quantitated using the comparative C_T method. Primers are in Supporting Information Table S1.

Patient tissue samples

The study cohort contained tissue samples from 66 BCa cases obtained from the Breast Cancer Campaign Tissue Bank under tissue request number TR000017. Patients provided consent to the Breast Cancer Campaign Tissue Bank for their tissues to be used for research. The samples came from women aged 28–89 years, who were diagnosed between

February 1992 and February 2012. For 40 cases (60%), tumour samples came with matched surrounding normal breast tissue. Clinical and histopathological data were available for all cases. Immunohistochemistry was performed on 5µm-thick sections using the EnVision+ System-HRP kit (Dako). Sections were deparaffinized in Histo-Clear (National Diagnostics) followed by antigen retrieval at 95°C for 30 min in Target Retrieval Solution (Dako). Sections were incubated with anti-β1 antibody (1:25; Abgent) for 30 mins and counterstained with dilute Mayer's hematoxylin and mounted in Faramount medium (Dako). Slides were scanned at 40× using an Aperio ScanScope. β1 immunoreactivity was scored by two independent investigators (WJB and RMS, a breast histopathologist) using the Allred method.²⁸ Briefly, the proportion of β1-positive cells was given a score (none: 0; <1/100: 1; 1/100 to 1/10: 2; 1/10 to 1/3: 3; 1/3 to 2/3: 4; >2/3: 5), followed by the intensity of staining (none: 0; weak: 1; intermediate: 2; strong: 3). For each section, the proportion and intensity scores were summed to give a total score (0–8). A score of 0–4 was considered “low” and 5–8 was considered “high.” Scoring was performed without prior knowledge of outcome data. Experiments were approved by the University of York Ethical Review Process.

Western blotting

SDS-PAGE was performed as described.^{15,29} The following antibodies were used: rabbit anti-β1 (1:100; Abgent), mouse anti-fyn (1:1,000; BioLegend), mouse anti-CD44 (1:1,000; AbD Serotec); rabbit anti-E-cadherin (1:1,000; Cell Signaling Technology); mouse anti-β-actin (1:30,000; Proteintech); and mouse anti-α-tubulin (1:10,000; Sigma). Signals were quantified using ImageJ software. α-tubulin was used as loading control.

Orthotopic breast tumour model

All animal procedures were carried out after approval by the University of York Ethical Review Process and under authority of a UK Home Office Project Licence. Six-week-old female *Rag2*^{-/-} *Il2rg*^{-/-} mice (mean weight: 16.6 ± 0.2 g) were obtained from the Yorkshire Cancer Research Unit, University of York. Mice (4–5 per specific pathogen free cage) were selected at random for surgery. A 1 × 10⁶ control MDA-MB-231-GFP or MDA-MB-231-β1-GFP cells expressing luciferase were suspended in Matrigel (20% v/v in saline) and injected into the left and right inguinal mammary fat pad of each animal whilst under isoflurane anaesthesia. A total of 13 mice were used (six injected with control cells and seven with β1 cells) across three independent replicated experiments. Tumour growth was monitored weekly by bioluminescence imaging. Mice were given intraperitoneal injection of D-luciferin in PBS (150 mg kg⁻¹) and bioluminescence was visualized 10 min later under isoflurane anaesthesia using an IVIS100 system (PerkinElmer). Bioluminescence from tumours was quantified within manually defined regions of interest using Living

Image software (PerkinElmer) and expressed as photon flux. To quantify bioluminescence at sites of metastasis, mice were euthanized ~10 min after injection with D-luciferin, primary tumours were removed and internal organs were exposed by dissection. Bioluminescence was measured from the entire mouse and then individual organs were removed for separate imaging. Measurements of the length and width of each tumour (in mm) were taken from mice daily with callipers. Tumour volume was calculated as 0.5 × (length × width²). Mice were euthanized when primary tumours reached 10% of starting body weight, or at the first sign of discomfort from metastatic burden. Tumours and organ sites of metastasis were fixed in 4% paraformaldehyde and frozen.¹⁴

Immunohistochemistry (IHC) and immunocytochemistry (ICC)

For H&E staining, sections were stained with Gill's hematoxylin and eosin Y and then scanned at 20X using a Zeiss AxioScan.Z1 slide scanner. The following primary antibodies were used for IHC/ICC¹⁵: rabbit anti-Ki67 (1:5,000; Abcam); rabbit anti-activated caspase-3 (1:200; R&D Systems); rabbit anti-CD31 (Santa Cruz Biotechnology); mouse anti-skeletal myosin (1:400; Sigma); rabbit anti-β1 (1:200; Abgent); mouse anti-fyn (1:100; BioLegend); mouse anti-CD44 (1:100; AbD Serotec); rabbit anti-E-cadherin (1:200; Cell Signaling Technology); mouse anti-human nuclear antigen (HNA; 1:100; Millipore). Secondary antibodies were Alexa-568-conjugated goat anti mouse/rabbit, unless stated otherwise (1:500; Invitrogen). Samples were mounted in Prolong Gold with DAPI (Invitrogen). Some samples were stained with Alexa-633-phalloidin (1:25; Invitrogen).²³ Samples were viewed using 20× objectives on a Nikon Eclipse TE200 fluorescent microscope, or Zeiss Axio Observer.Z1 microscope with LSM 710 confocal laser scanner.

Image analysis

Images were exported into ImageJ for processing. Confocal Z-series projections were flattened using the maximum signal. Brightness/contrast was adjusted using the ImageJ “Auto” function. ICC colocalization was evaluated using ImageJ. Intensity correlation analysis (ICA) was performed on individual cells delineated with the freehand selection tool, and for each cell, the intensity correlation quotient (ICQ) was computed. For signal intensities that vary together, indicating colocalization, 0 < ICQ ≤ 0.5, whereas for segregated staining, -0.5 ≤ ICQ < 0.³⁰ Measurements were from 20 cells per line.

The following measurements were made on IHC sections, for three mice per treatment group:

- Density of Ki67⁺ or activated caspase-3⁺ cells¹⁷: the number of Ki67⁺ nuclei or active caspase-3⁺ cells was counted per 20X field of view.

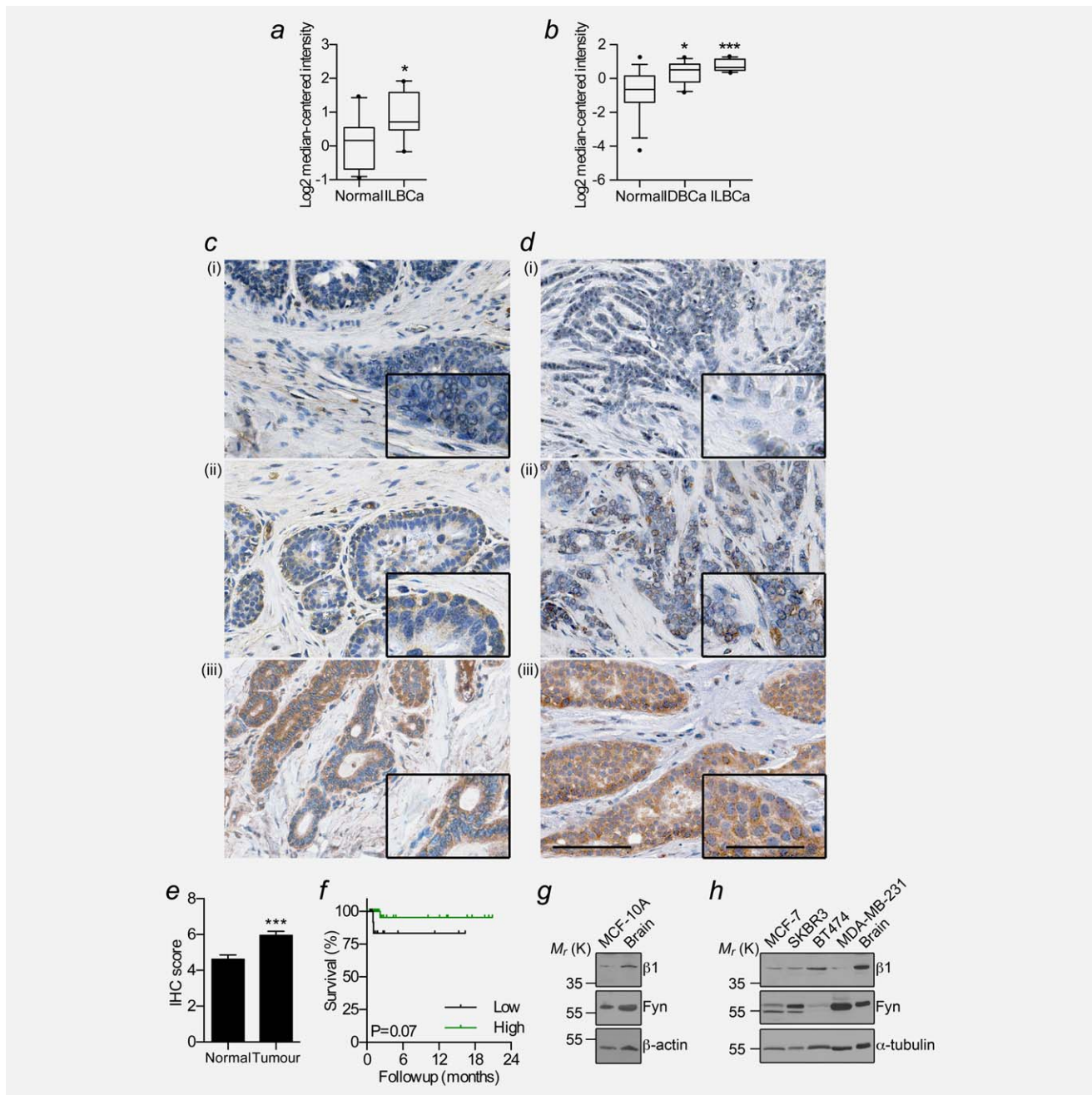


Figure 1. $\beta 1$ mRNA and protein expression in breast cancer. (a) Expression of *SCN1B* mRNA in invasive lobular breast carcinoma (ILBCa) vs. normal in the Radvanyi Breast dataset ($n = 15$). (b) Expression of *SCN1B* in invasive ductal breast cancer (IDBCa) and ILBCa in the Turashvili Breast dataset ($n = 30$). Box plot dots, maximum and minimum values; whiskers, 90th and 10th percentile values; and horizontal lines, 75th, 50th, and 25th percentile values. (c) Representative images of non-cancer breast tissue and (d) breast tumour tissue in which $\beta 1$ was (i) absent, (ii) weakly positive, and (iii) strongly positive. Scale bar, 100 μm . Insets, higher magnification images of tumour cells, scale bar, 50 μm . (e) Mean Allred score for normal breast and tumour samples. Data are mean \pm SEM ($n = 66$). (f) Kaplan–Meier analysis comparing BCa-specific survival of those with “low” (score < 5) vs. “high” (score ≥ 5) $\beta 1$ expression ($n = 62$). (g) Western blot of $\beta 1$ and fyn in the MCF-10A non-cancer mammary epithelial cell line. (h) Western blot of $\beta 1$ and fyn across a panel of BCa cell lines. Positive control = rat brain lysate. * $p < 0.05$; ** $p < 0.01$; *** $p < 0.001$.

- Tumour vascularity³¹: the number of CD31⁺ vessels was counted per 20X field of view.
- Metastasis to liver/lungs/spleen³²: the number of GFP⁺ metastatic foci was counted per 20X field of view.
- Length of tumour cell processes and muscle fibers: The longest visible process on cancer cells and the total length of individual muscle fibers within 20 \times fields of view was measured using the freeform line function in ImageJ.

VEGF ELISA

Cells were cultured in 24-well plates (5×10^4 /well). After 1, 2, and 3 days, culture medium was removed from individual wells and stored at -20°C until analysis. VEGF secretion was determined by ELISA (Promega). Measurements were obtained from duplicate wells from three repeat experiments.

Process outgrowth assay

Process outgrowth assays were based on Ref. 14. Parental CHL fibroblasts or CHL fibroblasts expressing $\beta 1$ were grown to confluence on 13mm diameter coverslips. Freshly dissociated BCa cells were plated (2×10^4 cells/well) on top of the monolayers and allowed to grow for 24–48 h. Cultures were fixed in 4% paraformaldehyde and the cancer cells were visualized with anti-GFP (1:1,000; NeuroMab), or anti-cytokeratin 18 (1:500; BioLegend) followed by Alexa-568-conjugated goat anti-mouse (1:500). Images were acquired using a Nikon Eclipse TE200 fluorescent microscope with $40\times$ objective. The longest process on each of the first 50 randomly selected, isolated cancer cells was measured using ImageJ. Measurements were obtained from three independent experiments.

Deletion of $\beta 1$ Ig domain

The Ig domain of $\beta 1$ (amino acids 40–124) in pEGFPN1²⁴ was deleted using the Phusion site-directed mutagenesis kit (Thermo Scientific). The $\beta 1\Delta_{40-124}$ -GFP construct was sequenced, and then transfected into MDA-MB-231 cells using Fugene (Roche).²⁴

RNA interference

SiGENOME SMARTpool siRNA targeting *FYN* and siGENOME Non-Targeting siRNA Pool #1 (Dharmacon) were used at 50 nM. Transfection was performed using Dharmafect 1 reagent. Transfection efficiency was confirmed to be $\geq 90\%$ using siGENOME positive control targeting *GAPDH* (Supporting Information Fig. S5c). RNA extraction and process outgrowth assay were performed 96h after transfection.

Data analysis

Data are mean and SEM unless stated otherwise. Statistical analysis was performed using GraphPad Prism. Matrix data were plotted using Matrix2png software.³³ Statistical significance was determined with *t* tests or Mann–Whitney tests, and multiple comparisons were made using ANOVA and Tukey *post hoc* tests, unless stated otherwise. *p* values computed by Oncomine were corrected for multiple comparisons by Bonferroni method. Correlation between *ESR1* and *SCN1B* expression was determined using Pearson's *r* test. Association between categorical classification criteria was determined with Fisher's exact test, or χ^2 test. For meta-analysis of association between *SCN1B* expression and histoclinical characteristics across multiple datasets, the binomial test was used.²⁶ The binomial test *p* value indicates whether or not

one criterion was associated with another in the observed number of datasets by chance, given the number of datasets studied. Kaplan–Meier curves for survival were compared by log-rank tests. Percent survival and hazard ratios are presented with 95% confidence intervals. Results were considered significant at $p < 0.05$.

Results

$\beta 1$ mRNA and protein are present in breast tumours

We have previously shown that $\beta 1$ mRNA/protein are expressed in BCa cell lines.²⁴ Here, we used Oncomine to study the expression of *SCN1B* mRNA in normal breast and BCa specimens across multiple microarrays. *SCN1B* was expressed at a significantly higher level in BCa compared with normal breast in two out of eight datasets in which differential data were available (1.7-fold, $p < 0.05$; and > 2.2 -fold, $p < 0.05$; Figs. 1a and 1b). We next performed a meta-analysis to investigate whether *SCN1B* expression correlates with histoclinical characteristics across multiple datasets. High *SCN1B* expression associated with ER status in 8/21 (38.1%) of datasets ($p < 0.0001$; Supporting Information Table S2; Figs. S1a and S1b). There was no significant association between *SCN1B* and age, pathological tumour size, grade, recurrence, progesterone receptor, or HER2 status across the same datasets. Up-regulation of *SCN1B* expression in ER⁺ tumours correlated with several genomic neighbours on chromosome 19q (Supporting Information Fig. S1c).²⁶ However, mRNA levels of the two *SCN1B* splice variants, $\beta 1$ and $\beta 1B$,³⁴ which are both expressed across a panel of BCa cell lines (Supporting Information Figs. S1d and S1e), were unchanged in MCF-7 cells following treatment with estrogen or fulvestrant (Supporting Information Fig. S1f), suggesting that *SCN1B* is not estrogen-regulated.

We next studied the expression of $\beta 1$ at protein level in human tissue samples by IHC. $\beta 1$ immunoreactivity was mainly in the cytoplasm of epithelial and carcinoma cells, with variable expression at the plasma membrane (Figs. 1c and 1d). This pattern of expression is consistent with previous observations in neurons and cancer cell lines.^{14,16,23} $\beta 1$ expression was significantly higher in tumour than normal, non-cancer breast tissue samples ($p < 0.001$; Fig. 1e). Of the cases where tumour had matched surrounding non-cancer tissue, 27 (68%) had higher $\beta 1$ in tumour than non-cancer tissue, 7 (17%) had the same level of $\beta 1$ in tumour and non-cancer tissue, and 6 (15%) had lower expression in tumour than non-cancer tissue. $\beta 1$ expression in the tumour did not correlate with age, ER status, grade, menopausal status, or node status (Supporting Information Table S3). Similarly, there was no relationship with BCa-specific survival (Fig. 1f, Supporting Information Table S3). In agreement with the IHC data, $\beta 1$ was also expressed at protein level in the non-cancer mammary epithelial MCF-10A cell line and across a panel of BCa cell lines (Figs. 1g and 1h). Together, these data suggest that $\beta 1$ may be up-regulated in a unique subset of breast cancers at mRNA and protein level.

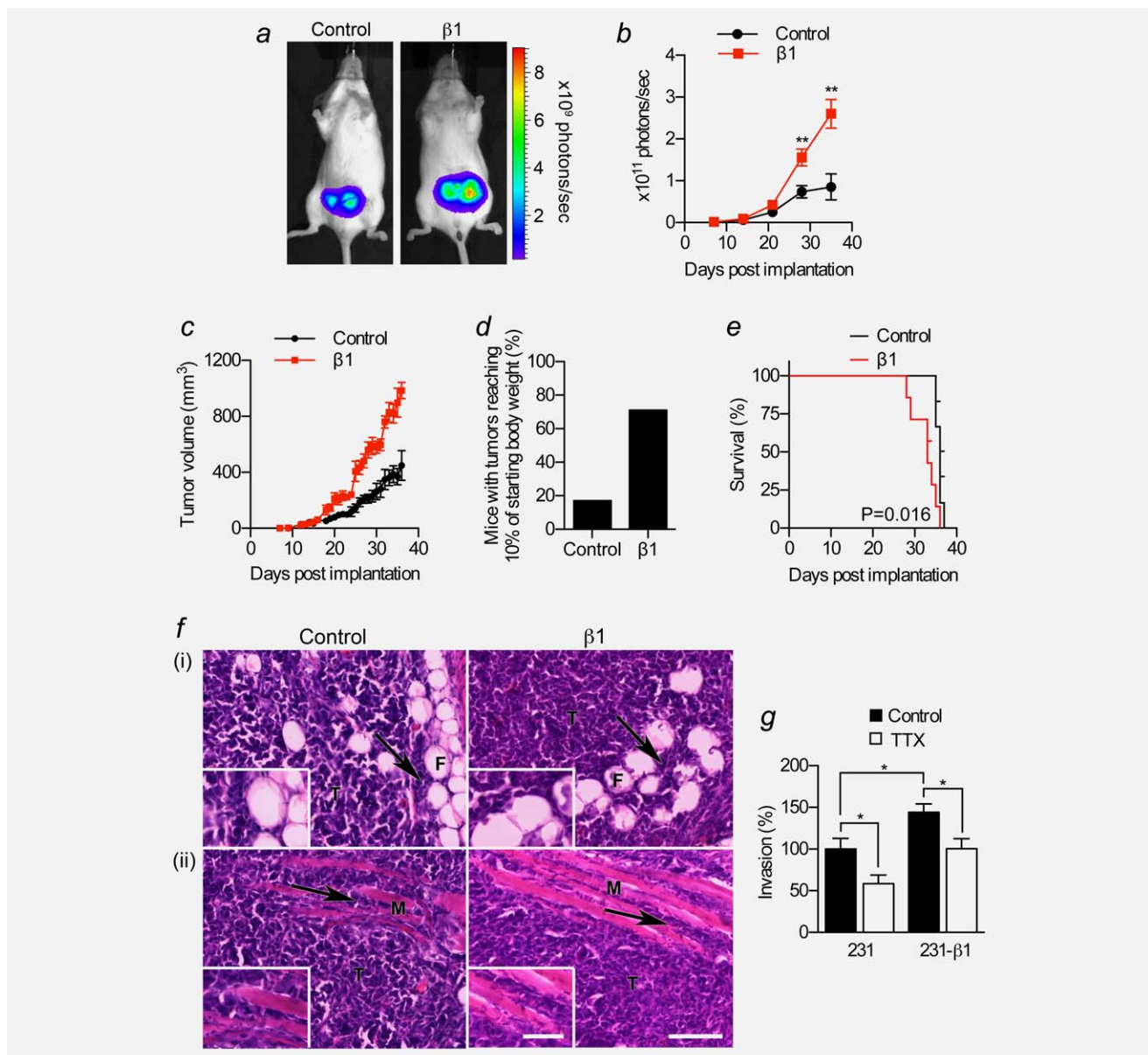


Figure 2. Effect of $\beta 1$ over-expression on breast tumour growth *in vivo*. MDA-MB-231 (“Control”) and MDA-MB-231- $\beta 1$ (“ $\beta 1$ ”) cells were implanted into the inguinal mammary fat pads of female *Rag2*^{-/-} *Il2rg*^{-/-} mice. (a) Representative bioluminescent images of mice bearing control and $\beta 1$ tumours, 4 weeks after implantation. (b) Bioluminescence measured from primary tumours on the indicated days post-implantation ($n \geq 12$). Data are mean \pm SEM; ** $p < 0.01$. (c) Calculated volume derived from calliper measurement of primary tumours over the same period ($n \geq 12$). (d) Percentage of mice whose primary tumour burden reached 10% of starting body weight within the 5-week tumour growth period is shown for control and $\beta 1$ tumours. (e) Kaplan–Meier analysis comparing overall survival of mice bearing control and $\beta 1$ tumours ($n = 13$). (f) Images of control and $\beta 1$ tumour tissue sections stained with H&E showing (i) mammary fat pad and (ii) skeletal muscle invasion. Arrows, infiltration of tumour cells (T) into fibroadipose tissue (F) or skeletal muscle fibers (M). Scale bar, 100 μ m. Insets, higher magnification images of invading tumour cells, scale bar, 50 μ m. (g) Invasion of control MDA-MB-231 and MDA-MB-231- $\beta 1$ cells \pm TTX (30 μ M) for 48 hr ($n = 12$; * $p < 0.05$; Neuman–Keuls test).

$\beta 1$ promotes tumour growth and vascularization

We next investigated the role of $\beta 1$ in tumour growth and metastasis. We orthotopically implanted luciferase-expressing MDA-MB-231 or MDA-MB-231- $\beta 1$ cells into the mammary fat pads of female *Rag2*^{-/-} *Il2rg*^{-/-} mice and monitored tumour growth by bioluminescent imaging. We chose this model because MDA-MB-231 cells rapidly form palpable

tumours following orthotopic implantation, and the cells readily metastasise. MDA-MB-231 cells express very low endogenous $\beta 1$ (Supporting Information Fig. S2a). By contrast, MDA-MB-231- $\beta 1$ cells over-express $\beta 1$ -GFP by >40-fold relative to endogenous $\beta 1$ (Supporting Information Figs. S2a and S2b).²⁴ Over-expression of $\beta 1$ had no effect on expression of CD44 or E-cadherin (Supporting Information

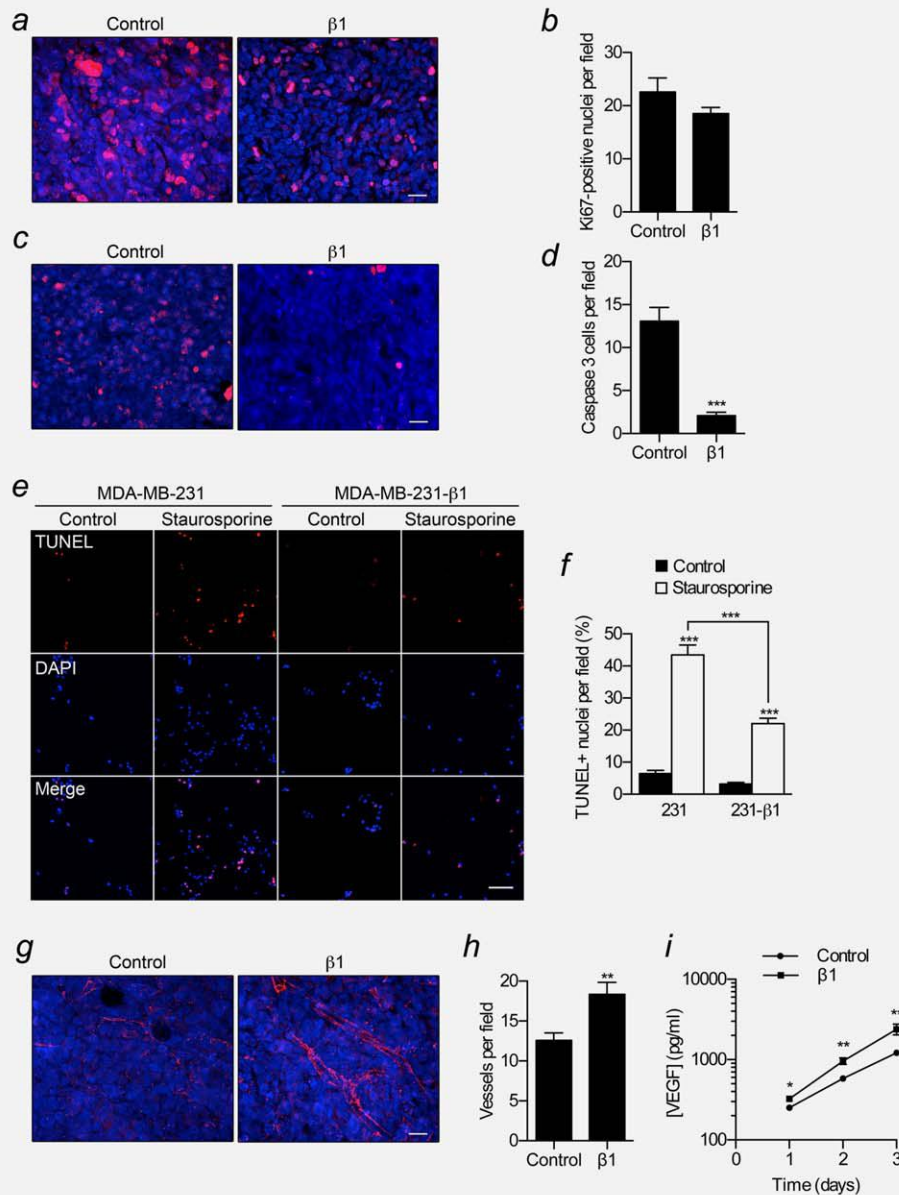


Figure 3. Effect of $\beta 1$ upregulation on proliferation, apoptosis and angiogenesis. (a) Control and $\beta 1$ tumour sections stained with anti-Ki67 (red) and DAPI (blue). Scale bar, 20 μm . (b) Ki67-positive nuclei per field of view for control and $\beta 1$ tumours ($n = 30$). (c) Control and $\beta 1$ tumour sections stained with anti-activated caspase-3 (red) and DAPI (blue). Scale bar, 20 μm . (d) Activated caspase-3-positive cells per field of view for control and $\beta 1$ tumours ($n = 30$). (e) Images of control and MDA-MB-231- $\beta 1$ cells treated for 24 hr with/without 0.5 μM staurosporine, analyzed by TUNEL assay (red), counterstained with DAPI (blue). Scale bar, 100 μm . (f) Proportion (%) of TUNEL-positive nuclei per field of view ($n = 60$). (g) Blood vessels stained with endothelial marker CD31 (red) and DAPI (blue) in control and $\beta 1$ tumour sections. Scale bar, 20 μm . (h) CD31-positive blood vessels per field of view for control and $\beta 1$ tumours ($n = 30$). (i) VEGF content of culture medium of control and MDA-MB-231- $\beta 1$ cells 1–3 days after plating ($n = 6$). Data are mean \pm SEM; ** $p < 0.01$; *** $p < 0.001$.

Figs. S2c–S2e). Importantly, luciferase activity and GFP expression were very similar in both cell lines (Supporting Information Figs. S3a–S3d). Photon flux from MDA-MB-231- $\beta 1$ tumours increased faster than control MDA-MB-231 tumours, becoming statistically significant after 4 weeks (Figs. 2a and 2b). To confirm the bioluminescent imaging data, we also analyzed tumour growth by daily calliper measurement. The volume of MDA-MB-231- $\beta 1$ tumours increased more

rapidly than MDA-MB-231 tumours, closely agreeing with the bioluminescent data (Fig. 2c). During the 5-week study period, MDA-MB-231- $\beta 1$ primary tumour burden reached 10% of starting body weight in 71% of mice, compared with only 17% for control tumours (Fig. 2d). The survival of mice bearing MDA-MB-231- $\beta 1$ tumours was significantly reduced compared to those bearing control tumours ($p < 0.05$; hazard ratio = 6.3 [1.4–27.8]; Fig. 2e). These data demonstrate that

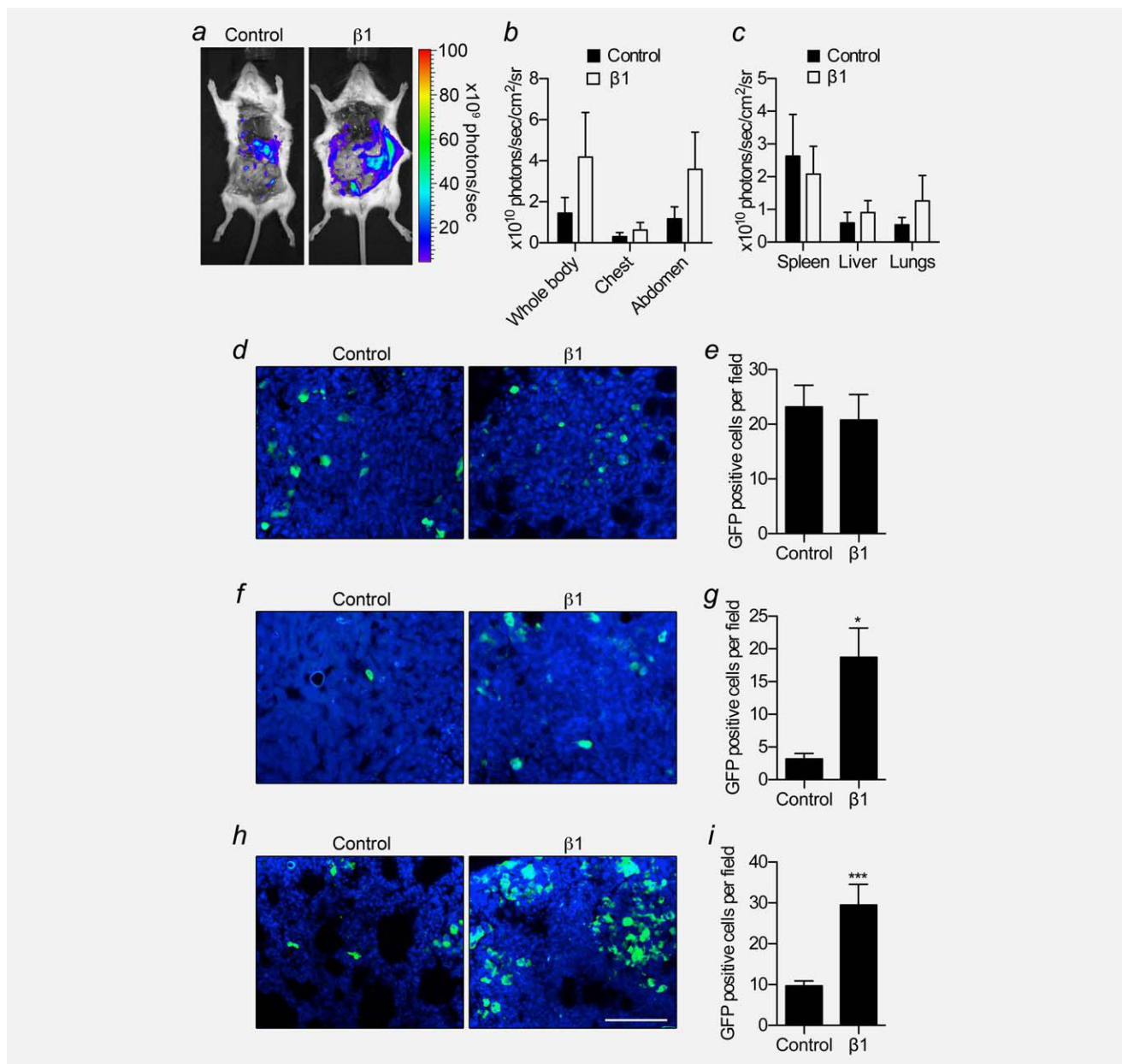


Figure 4. Effect of $\beta 1$ over-expression on breast cancer metastasis *in vivo*. At 5 weeks following implantation, control and $\beta 1$ tumours were removed *post mortem* prior to bioluminescent imaging. (a) Representative bioluminescent images of metastases from control and $\beta 1$ tumours. (b) Bioluminescence measured from the indicated anatomical sites from control and $\beta 1$ tumour-bearing mice ($n \geq 5$). (c) Bioluminescence measured *ex vivo* from the spleen, liver, and lungs of control and $\beta 1$ tumour-bearing mice ($n \geq 5$). (d) Spleen sections from control and $\beta 1$ tumour-bearing mice showing GFP signal (green) and DAPI (blue). (e) GFP-positive cells per field of view of spleen ($n = 30$). (f) Liver sections from control and $\beta 1$ tumour-bearing mice showing GFP signal (green) and DAPI (blue). (g) GFP-positive cells per field of view of liver ($n = 30$). (h) Lung sections from control and $\beta 1$ tumour-bearing mice showing GFP signal and DAPI (blue). (i) GFP-positive cells per field of view of lung ($n = 30$). Bars are mean + SEM; * $p < 0.05$; *** $p < 0.001$. Scale bar, 100 μm .

over-expression of $\beta 1$ enhanced the growth of breast tumours, thus reducing survival.

We next studied the structure and composition of the primary tumours. Both MDA-MB-231 and MDA-MB-231- $\beta 1$ tumours were broadly similar, containing some invasion into surrounding fibroadipose tissue and skeletal muscle (Fig. 2f). Although the *in vitro* invasiveness of MDA-MB-231- $\beta 1$ cells

was moderately higher than control MDA-MB-231 cells, blockade of α subunits with TTX inhibited invasion of both cell lines to a similar extent ($p < 0.05$, Fig. 2g). Thus, α -subunit-dependent invasion of MDA-MB-231 cells^{20,21} appears to be unaffected by $\beta 1$ over-expression. The density of Ki67⁺ cycling cells was unchanged in MDA-MB-231- $\beta 1$ tumours, compared to control tumours (Figs. 3a and 3b).

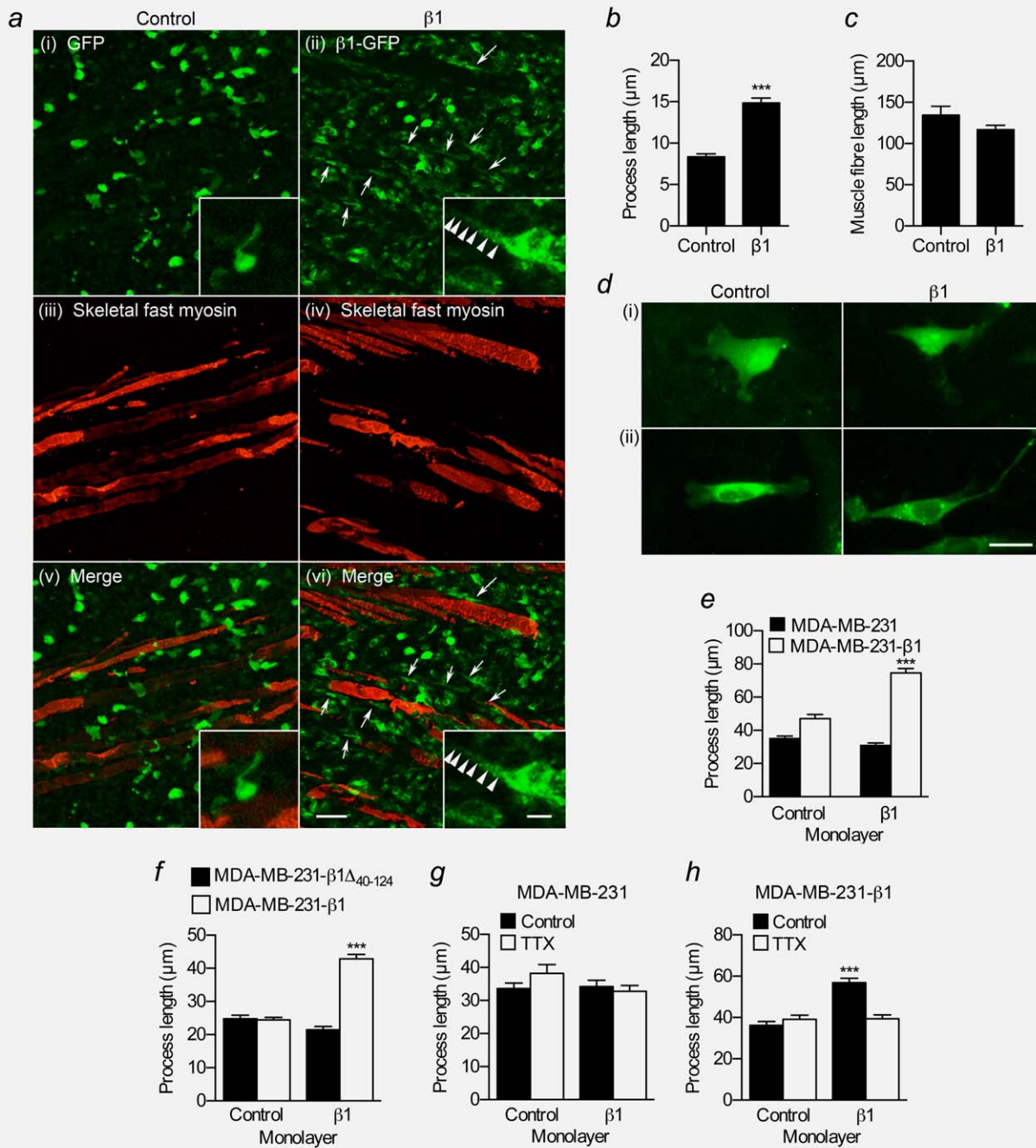


Figure 5. Effect of $\beta 1$ on process outgrowth in breast cancer cells. (a) Regions of skeletal muscle infiltration in control (i,iii,v) and $\beta 1$ (ii,iv,vi) tumour sections showing GFP signal (green) and skeletal fast myosin (red). Arrows indicate cells in $\beta 1$ tumours that have more elongate processes. Scale bar, 50 μm . Insets, higher magnification images of tumour cells showing processes. Inset scale bar, 10 μm . (b) Process length (μm) of control MDA-MB-231 and MDA-MB-231- $\beta 1$ cells in tumours ($n \geq 134$ cells/each). (c) Length (μm) of muscle fibers in control and $\beta 1$ tumours ($n \geq 79$). (d) Images of MDA-MB-231 and MDA-MB-231- $\beta 1$ cells grown on control or $\beta 1$ -expressing CHL fibroblast monolayers, and stained with anti-GFP antibody. Scale bar, 20 μm . (e) Process length (μm) of MDA-MB-231 and MDA-MB-231- $\beta 1$ cells grown on control or $\beta 1$ -expressing CHL monolayers ($n = 300$). (f) Process length (μm) of MDA-MB-231- $\beta 1\Delta_{40-124}$ and MDA-MB-231- $\beta 1$ cells grown on control or $\beta 1$ -expressing CHL monolayers ($n = 300$). (g) Process length (μm) of MDA-MB-231 cells grown on control or $\beta 1$ -expressing CHL monolayers $\pm 30 \mu\text{M}$ TTX ($n \geq 144$). (h) Process length (μm) of MDA-MB-231- $\beta 1$ cells grown on control or $\beta 1$ -expressing CHL monolayers $\pm 30 \mu\text{M}$ TTX ($n = 150$). Bars are mean + SEM; *** $p < 0.001$.

However, the density of apoptotic cells expressing activated caspase-3 was significantly reduced by 84% in MDA-MB-231- $\beta 1$ tumours, compared to control tumours ($p < 0.001$;

Figs. 3c and 3d). *In vitro*, staurosporine-induced apoptosis was significantly reduced in MDA-MB-231- $\beta 1$ cells, compared to control MDA-MB-231 cells (Figs. 3e and 3f),

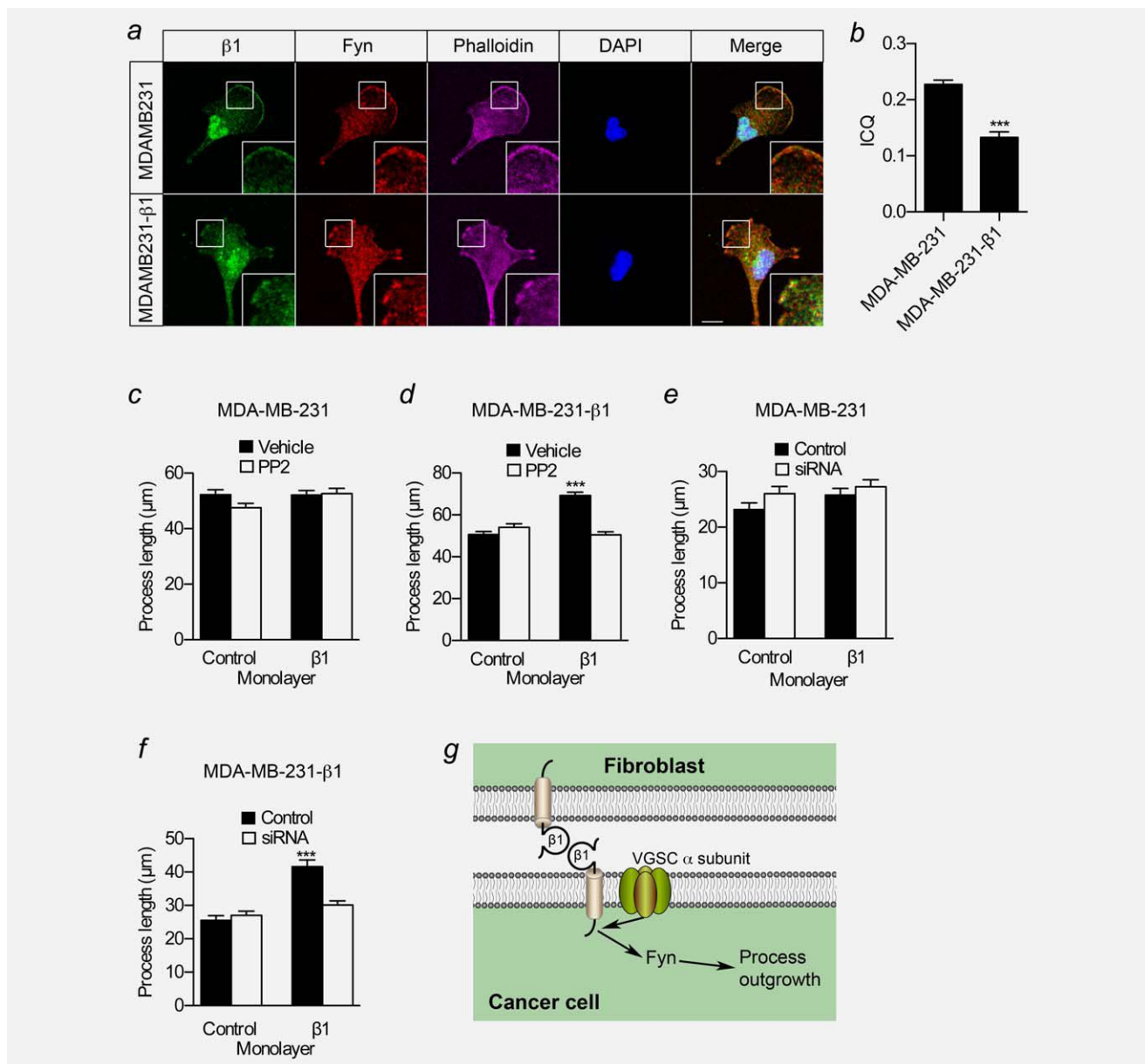


Figure 6. A mechanism for $\beta 1$ -mediated process outgrowth and migration in BCa cells. (a) Images of MDA-MB-231 and MDA-MB-231- $\beta 1$ cells. Green: anti- $\beta 1$ for parental MDA-MB-231 (with Alexa-488-conjugated secondary antibody) and GFP signal for MDA-MB-231- $\beta 1$; red: anti-fyn; magenta: phalloidin to label the actin cytoskeleton; blue: DAPI to label nucleus. White boxes indicate locations of inset zoomed images. Phalloidin is omitted from merged image for clarity. Scale bar, 10 μm . (b) Intensity correlation-quotients (ICQ) for $\beta 1$ and fyn in MDA-MB-231 and MDA-MB-231- $\beta 1$ cells ($n = 20$ /each). (c) Process length (μm) of MDA-MB-231 cells grown on control or $\beta 1$ -expressing CHL monolayers $\pm 5 \mu\text{M}$ PP2 ($n \geq 147$). (d) Process length (μm) of MDA-MB-231- $\beta 1$ cells grown on control or $\beta 1$ -expressing CHL monolayers $\pm 5 \mu\text{M}$ PP2 ($n \geq 223$). (e) Process length (μm) of MDA-MB-231 cells grown on control or $\beta 1$ -expressing CHL monolayers \pm fyn siRNA ($n = 150$). (f) Process length (μm) of MDA-MB-231- $\beta 1$ cells grown on control or $\beta 1$ -expressing CHL monolayers \pm fyn siRNA ($n = 150$). (g) A model of possible signalling mechanism underlying $\beta 1$ -mediated process outgrowth in BCa cells. $\beta 1$ from an adjacent fibroblast or cancer cell interacts in *trans* with $\beta 1$ on the BCa cell, initiating a signaling cascade via fyn kinase, leading to process outgrowth.¹⁵ Na^+ conductance through the pore-forming α subunit is also required.¹⁶ Figure was produced using Science Slides software. Bars are mean + SEM; *** $p < 0.001$.

suggesting, together with the tumour data, that $\beta 1$ overexpression enhances resistance to apoptosis. Finally, the density of vascular structures, revealed by labelling blood vessels with an antibody to the endothelial marker CD31, signifi-

cantly increased by 1.5-fold in MDA-MB-231- $\beta 1$ tumours, compared to control tumours, and VEGF secretion *in vitro* was significantly higher in MDA-MB-231- $\beta 1$ cells than control MDA-MB-231 cells ($p < 0.01$; Figs. 3g–3i). In summary,

these data suggest that $\beta 1$ over-expression increased the growth of MDA-MB-231 tumours, not by altering the density of cycling cells in the population, but, instead by reducing apoptosis and enhancing angiogenesis.

$\beta 1$ potentiates metastasis to liver and lungs

We monitored metastasis after 5 weeks by bioluminescent imaging following *post mortem* resection of primary tumours (Fig. 4a). Although photon flux was slightly increased in mice bearing MDA-MB-231- $\beta 1$ tumours compared those bearing MDA-MB-231 tumours, and in the liver and lungs *ex vivo*, this difference was not statistically significant (Figs. 4b and 4c). To study metastasis to these organs in more detail at the cellular level, using a more sensitive method, we measured the density of GFP-expressing tumour cells within tissue sections. We detected GFP⁺ cells in sections both in isolation, and in multicellular foci (Figs. 4d, 4f, and 4h). GFP was co-expressed in cells with HNA (Fig. S3e). HNA is present in human MDA-MB-231 cells, but absent in mouse cells, thus confirming that GFP expression was retained in the tumour cells once they had metastasized. In the spleen, the number of GFP⁺ cells per field of view was unchanged between groups (Fig. 4e). However, the number of GFP⁺ cells per field of view was significantly increased, by 5.9- and 3.0-fold, respectively, in the liver and lungs of MDA-MB-231- $\beta 1$ tumour-bearing mice, compared to control ($p < 0.05$ and 0.001, respectively; Figs. 4g and 4i). Thus, $\beta 1$ over-expression promoted metastasis to the liver and lungs, but not the spleen.

$\beta 1$ promotes process outgrowth

Enhancement of protrusions, *e.g.*, pseudopodia, from cells is associated with increased motility in 3D cultures, invasion, and metastasis.^{35–37} Over-expression of $\beta 1$ in MDA-MB-231 cells increases the length of processes protruding from the cell body *in vitro*.²⁴ We therefore postulated that $\beta 1$ might regulate cellular morphology in our tumour model. In the periphery of tumour sections, MDA-MB-231- $\beta 1$ cells infiltrating surrounding skeletal muscle appeared more densely packed, and had a more elongate morphology than MDA-MB-231 cells (Fig. 5a). In these sections, processes extending from MDA-MB-231- $\beta 1$ cells were significantly longer than processes on MDA-MB-231 cells (Fig. 5b). The length of muscle fibers was unchanged between tumour types (Fig. 5c).

In the nervous system, $\beta 1$ regulates neuronal morphology and neurite outgrowth *via trans-homophilic* adhesion.¹⁵ We therefore set out to test the hypothesis that this neuronal function of $\beta 1$ is recapitulated when it is expressed in BCa cells, enhancing process outgrowth. We examined the morphology of BCa cells plated on monolayers of control and $\beta 1$ -expressing CHL fibroblasts. CHL cells were chosen because they do not express endogenous β subunits.¹⁴ When plated on CHL cells, MDA-MB-231 cells produced thin processes with foci at the tips, morphologically similar to neurites with growth cones (Fig. 5d).¹⁵ MDA-MB-231 cells did not

show any increase in process length when grown on $\beta 1$ -expressing monolayers (Fig. 5e). However, MDA-MB-231- $\beta 1$ cells did respond, such that $\beta 1$ -expressing monolayers increased process length by 1.6-fold ($p < 0.001$; Fig. 5e). A similar result was observed for MCF-7 cells, which express endogenous $\beta 1$ (Supporting Information Fig. S4a and S4b). There was no increase in process length of MDA-MB-231 cells over-expressing the Ig domain-deficient mutant $\beta 1\Delta_{40-124}$ when grown on $\beta 1$ -expressing monolayers (Fig. 5f), suggesting that the adhesion domain is required for $\beta 1$ -mediated process outgrowth. In cerebellar granule neurons, $\beta 1$ -mediated neurite outgrowth requires the presence of Na_v1.6 and is inhibited by the VGSC pore-blocking toxin TTX.¹⁶ We found that TTX (30 μM) inhibited $\beta 1$ -mediated process outgrowth in MDA-MB-231- $\beta 1$ cells ($p < 0.001$; Fig. 5h). However, it had no effect on process outgrowth in native MDA-MB-231 cells, which do not respond to $\beta 1$ -expressing fibroblasts (Fig. 5g). Together, these data suggest that $\beta 1$ enhances process outgrowth on BCa cells *via trans-homophilic* adhesion between $\beta 1$ expressed on the BCa cell, and $\beta 1$ expressed on the adjacent fibroblast, similar to its function in neurons.¹⁴

$\beta 1$ -mediated process outgrowth requires fyn kinase

In neurons, $\beta 1$ increases neurite length *via* fyn kinase.¹⁵ CAM-mediated activation of fyn kinase is proposed to initiate the fyn-focal adhesion kinase (FAK) pathway, activating extracellular signal-regulated kinase 1/2, leading to neurite outgrowth.³⁸ Fyn is upregulated in a number of cancers, where it contributes to an invasive phenotype.³⁹ We found that fyn, like $\beta 1$, was expressed in MCF-10A cells and BCa cell lines (Fig. 1g and 1h, Supporting Information Fig. S2f). Given that fyn is required for $\beta 1$ -mediated neurite outgrowth, and fyn and $\beta 1$ are coexpressed in brain membranes,¹⁵ we hypothesized that fyn and $\beta 1$ may colocalize in BCa cells. In MDA-MB-231 and MDA-MB-231- $\beta 1$ cells, $\beta 1$ was expressed throughout the cytoplasm, on perinuclear internal membranes and lamellipodia (Fig. 6a), consistent with previous observations, although the expression of $\beta 1$ was clearly lower in the former.²³ Importantly, fyn showed a broadly similar distribution to $\beta 1$, with expression strongest on F-actin-rich lamellipodia. Intensity correlation analysis gave ICQ values > 0 , indicating that the signals for $\beta 1$ and fyn varied together³⁰ (Fig. 6b). This result is consistent with $\beta 1$ colocalizing with fyn.

We next investigated whether fyn activity is involved in $\beta 1$ -mediated process outgrowth in BCa cells. Inclusion of the src family kinase inhibitor PP2 (5 μM) in the assay inhibited $\beta 1$ -mediated process outgrowth in MDA-MB-231- $\beta 1$ cells ($p < 0.001$; Fig. 6d). However, it had no effect on process outgrowth in control MDA-MB-231 cells, which do not respond to $\beta 1$ -expressing fibroblasts (Fig. 6c). Importantly, 5 μM PP2 had no effect on cellular viability or proliferation (Supporting Information Figs. S5a and S5b). To establish whether fyn is specifically required for $\beta 1$ -mediated process outgrowth in

BCa cells over other members of the src family that are also inhibited by PP2, we next transiently down-regulated the expression of fyn in BCa cells using siRNA, prior to plating on fibroblast monolayers (Supporting Information Fig. S5d). Down-regulation of fyn with siRNA abrogated $\beta 1$ -mediated process outgrowth in MDA-MB-231- $\beta 1$ cells ($p < 0.001$; Fig. 6f). However, there was no effect on baseline process outgrowth in control MDA-MB-231 cells (Fig. 6e). PP2 and fyn siRNA also inhibited $\beta 1$ -mediated process outgrowth in MCF-7 cells (Supporting Information Figs. S4c and S4d). In summary, blocking fyn expression/activity with PP2 or siRNA inhibited $\beta 1$ -mediated process outgrowth in BCa cells. These data suggest that fyn is a critical signalling intermediary in the mechanism underlying $\beta 1$ -mediated process outgrowth in BCa cells (Fig. 6g), as it is in neurons.¹⁵

Discussion

VGSCs are expressed in cells from a number of different cancers, where they are proposed to play a role in potentiating metastasis.¹⁸ VGSCs are unique among ion channels in that their “auxiliary” β subunits not only modulate channel activity, but are also CAMs.⁵ Expression of β subunits has been reported in breast, bone, cervical, colorectal, lung, and prostate cancer cell lines, and $\beta 1$ is the dominant isoform in breast, cervical, lung and prostate cancer cell lines (reviewed in Ref. 19). However, *in vivo* evidence for β subunit expression in cancer is limited. We found that $\beta 1$ was up-regulated at mRNA and protein level in BCa specimens compared with non-cancer tissue. Similarly, $\beta 1$ was expressed across a panel of BCa cell lines, although the relative mRNA and protein levels differed. In addition, in tumour specimens, the positive relationship between *SCN1B* mRNA and ER status was not reflected at the protein level. Discrepancy between mRNA and protein levels has been reported previously for other VGSCs in other tissues.^{24,40,41} Therefore, the relationship between *SCN1B* mRNA and $\beta 1$ protein levels may be subject to complex regulation, highlighting the critical importance of studying biomarker expression at both mRNA and protein levels. We did not observe a relationship between $\beta 1$ expression and outcome in patient tumour specimens. This may be due to the relatively small size of the dataset, and it would be worthwhile in the future to validate the data presented here against larger cohorts. In conclusion, our data show that *SCN1B*/ $\beta 1$ is up-regulated at the mRNA and protein level in BCa. We propose that $\beta 1$ warrants further study as a potential biomarker for BCa.

$\beta 1$ over-expression increased tumour growth *in vivo*. Interestingly, this contrasts with the observation that over-expression of $\beta 1$ slightly reduces proliferation *in vitro*,²⁴ suggesting that the tumour microenvironment might be critical to the *in vivo* tumour-promoting function of $\beta 1$. In support of this, apoptosis was reduced in MDA-MB-231- $\beta 1$ tumours, which may account for their increased size. Cell adhesion can promote apoptosis suppression in cancer cells via FAK activation⁴² and further work is required to establish whether or

not $\beta 1$ -dependent adhesion promotes tumour cell survival. There was increased density of vascular structures in the $\beta 1$ over-expressing tumours, and VEGF secretion was increased in MDA-MB-231- $\beta 1$ cells *in vitro*, suggesting that $\beta 1$ may enhance angiogenesis. Several classes of CAMs are known to promote angiogenesis, including integrins, cadherins, and immunoglobulin superfamily CAMs,⁴³ raising the possibility that $\beta 1$ may contribute to promoting blood vessel development through heterophilic adhesion. Interestingly, over-expression of $\beta 2$ in prostate cancer cells has the reverse effect, reducing tumour growth.⁴⁴ Despite its structural similarity to $\beta 1$, $\beta 2$ appears to play a different role in the CNS, and is not essential for postnatal development.⁵ Thus, as in the CNS, different β subunits may perform distinct functions in different cancer microenvironments.

$\beta 1$ is a multifunctional molecule that plays a critical role during CNS development.⁵ Although $\beta 1$ is essential for regulating excitability through fine-tuning VGSC gating and kinetics,¹⁶ its function as a CAM is required for neurite outgrowth, migration, fasciculation and synaptic connectivity.^{15–17} In fact, $\beta 1$ may function as a CAM, independent of channel activity under certain conditions.⁵ Other CAMs that regulate neuronal migration and pathfinding have been reported in tumours, where they play a pathological role and associate with poor prognosis.⁴⁵ It is therefore not unreasonable to expect that $\beta 1$ may do the same. We showed previously that $\beta 1$ enhances cell-cell adhesion and cell-substrate adhesion in BCa cells *in vitro*.²⁴ In the present study, we found that $\beta 1$ over-expression in MDA-MB-231 cells caused a more elongate cellular morphology within tumours, and enhanced process outgrowth *in vitro via trans-homophilic* adhesion. $\beta 1$ -mediated process outgrowth did not occur in control MDA-MB-231 cells, which express a low level of endogenous $\beta 1$. The latter result suggests that $\beta 1$ expression on the tumour cell may need to be above a threshold in order to induce process outgrowth and enhance tumour growth and metastasis. We found that, as in neurons,¹⁵ $\beta 1$ -mediated process outgrowth in BCa cells required fyn kinase. $\beta 1$ -mediated neurite outgrowth in neurons is also activity-dependent.¹⁶ Interestingly, Na^+ current promotes src family kinase activity and pro-invasive morphology in MDA-MB-231 cells,⁴⁶ which fits with other data showing that α subunits potentiate the invasiveness of BCa cells.^{20–22,46,47} We found that TTX inhibited $\beta 1$ -mediated process outgrowth in MDA-MB-231- $\beta 1$ cells, suggesting that, as in neurons,¹⁶ α subunit function is required (Fig. 6g). Thus, $\text{Na}_v1.5$ and $\beta 1$ may both promote mesenchymal-like elongate morphology in BCa cells, *via* a combination of Na^+ current and adhesion.

Our data suggest that $\beta 1$ can enhance tumour growth and metastasis *via a trans-homophilic* adhesion mechanism that enhances process outgrowth on metastatic tumour cells, enabling their dissemination from the primary tumour and into surrounding tissues. This would fit with the observation that outgrowth of processes, *e.g.*, pseudopodia, from cancer cells increases motility, invasion, and metastasis.^{35–37} Thus, $\beta 1$

may be involved in collective cell migration and invasion during tumour spreading,^{48,49} similar to its role in pathfinding and fasciculation during CNS development.^{15,17} However, we do not yet know whether $\beta 1$ interactions in *trans* occur between adjacent tumour cells, or between tumour cells and stromal cells, or both. Further complexity is added by the possibility that $\beta 1$ may interact heterophilically with other CAMs,^{9–12} and/or extracellular matrix proteins¹³ present in the tumour microenvironment, dependent on cell types/status within the tumour.

Our data support the hypothesis that *SCN1B*/ $\beta 1$ recapitulates its neurodevelopmental role to promote breast tumour growth and metastasis. This fits with a growing body of evi-

dence implicating VGSCs as mediators of an invasive/metastatic phenotype.¹⁹ Up-regulation of genes, *e.g.* *SCN1B*, required for normal migration and invasion processes during development, may represent a critical event in the progression towards metastasis.⁵⁰ We therefore propose that (i) $\beta 1$ may represent a novel biomarker during disease development, and (ii) targeting $\beta 1$ -mediated adhesion interactions may have potential as novel anti-cancer therapy.

Acknowledgements

The authors acknowledge the role of the Breast Cancer Campaign Tissue Bank in collecting and making available the samples used in the generation of this publication.

References

- Autier P, Boniol M, La Vecchia C, et al. Disparities in breast cancer mortality trends between 30 European countries: retrospective trend analysis of WHO mortality database. *BMJ (Clin Res Ed)* 2010;341:c3620.
- Jemal A, Bray F, Center MM, et al. Global cancer statistics. *CA Cancer J Clin* 2011;61:69–90.
- Steeg PS, Theodorescu D. Metastasis: a therapeutic target for cancer. *Nat Clin Pract Oncol* 2008;5:206–219.
- Catterall WA. From ionic currents to molecular mechanisms: the structure and function of voltage-gated sodium channels. *Neuron* 2000;26:13–25.
- Brackenbury WJ, Isom LL. Na channel beta subunits: overachievers of the ion channel family. *Front Pharmacol* 2011;2:53.
- Kim DY, Carey BW, Wang H, et al. BACE1 regulates voltage-gated sodium channels and neuronal activity. *Nat Cell Biol* 2007;9:755–64.
- Malhotra JD, Kazen-Gillespie K, Hortsch M, et al. Sodium channel β subunits mediate homophilic cell adhesion and recruit ankyrin to points of cell-cell contact. *J Biol Chem* 2000;275:11383–8.
- Malhotra JD, Koopmann MC, Kazen-Gillespie KA, et al. Structural requirements for interaction of sodium channel $\beta 1$ subunits with ankyrin. *J Biol Chem* 2002;277:26681–8.
- Kazarinova-Noyes K, Malhotra JD, McEwen DP, et al. Contactin associates with Na^+ channels and increases their functional expression. *J Neurosci* 2001;21:7517–25.
- Malhotra JD, Thyagarajan V, Chen C, et al. Tyrosine-phosphorylated and nonphosphorylated sodium channel $\beta 1$ subunits are differentially localized in cardiac myocytes. *J Biol Chem* 2004;279:40748–54.
- Ratcliffe CF, Westenbroek RE, Curtis R, et al. Sodium channel $\beta 1$ and $\beta 3$ subunits associate with neurofascin through their extracellular immunoglobulin-like domain. *J Cell Biol* 2001;154:427–34.
- McEwen DP, Isom LL. Heterophilic interactions of sodium channel $\beta 1$ subunits with axonal and glial cell adhesion molecules. *J Biol Chem* 2004;279:52744–52.
- Xiao ZC, Ragsdale DS, Malhotra JD, et al. Tenascin-R is a functional modulator of sodium channel $\beta 1$ subunits. *J Biol Chem* 1999;274:26511–7.
- Davis TH, Chen C, Isom LL. Sodium channel $\beta 1$ subunits promote neurite outgrowth in cerebellar granule neurons. *J Biol Chem* 2004;279:51424–32.
- Brackenbury WJ, Davis TH, Chen C, et al. Voltage-gated Na^+ channel $\beta 1$ subunit-mediated neurite outgrowth requires fyn kinase and contributes to central nervous system development in vivo. *J Neurosci* 2008;28:3246–56.
- Brackenbury WJ, Calhoun JD, Chen C, et al. Functional reciprocity between Na^+ channel Nav1.6 and $\beta 1$ subunits in the coordinated regulation of excitability and neurite outgrowth. *Proc Natl Acad Sci USA* 2010;107:2283–8.
- Brackenbury WJ, Yuan Y, O'Malley HA, et al. Abnormal neuronal patterning occurs during early postnatal brain development of *Scn1b*-null mice and precedes hyperexcitability. *Proc Natl Acad Sci USA* 2013;110:1089–94.
- Fraser SP, Ozerlat-Gunduz I, Brackenbury WJ, et al. Regulation of voltage-gated sodium channel expression in cancer: hormones, growth factors and auto-regulation. *Philos Trans R Soc Lond Ser B Biol Sci* 2014;369:20130105.
- Brackenbury WJ. Voltage-gated sodium channels and metastatic disease. *Channels (Austin)* 2012;6:352–61.
- Fraser SP, Diss JK, Chioni AM, et al. Voltage-gated sodium channel expression and potentiation of human breast cancer metastasis. *Clin Cancer Res* 2005;11:5381–9.
- Roger S, Besson P, Le Guennec JY. Involvement of a novel fast inward sodium current in the invasion capacity of a breast cancer cell line. *Biochim Biophys Acta* 2003;1616:107–11.
- Gillet L, Roger S, Besson P, et al. Voltage-gated sodium channel activity promotes cysteine cathepsin-dependent invasiveness and colony growth of human cancer cells. *J Biol Chem* 2009;284:8680–91.
- Yang M, Kozminski DJ, Wold LA, et al. Therapeutic potential for phenytoin: targeting Na^+ channels to reduce migration and invasion in metastatic breast cancer. *Breast Cancer Res Treat* 2012;134:603–15.
- Chioni AM, Brackenbury WJ, Calhoun JD, et al. A novel adhesion molecule in human breast cancer cells: voltage-gated Na^+ channel $\beta 1$ subunit. *Int J Biochem Cell Biol* 2009;41:1216–27.
- Tomlins SA, Rhodes DR, Perner S, et al. Recurrent fusion of *TMPRSS2* and *ETS* transcription factor genes in prostate cancer. *Science* 2005;310:644–8.
- Rhodes DR, Ateeq B, Cao Q, et al. *AGTR1* overexpression defines a subset of breast cancer and confers sensitivity to losartan, an *AGTR1* antagonist. *Proc Natl Acad Sci USA* 2009;106:10284–9.
- Mycielska ME, Palmer CP, Brackenbury WJ, et al. Expression of Na^+ -dependent citrate transport in a strongly metastatic human prostate cancer PC-3M cell line: regulation by voltage-gated Na^+ channel activity. *J Physiol* 2005;563:393–408.
- Harvey JM, Clark GM, Osborne CK, et al. Estrogen receptor status by immunohistochemistry is superior to the ligand-binding assay for predicting response to adjuvant endocrine therapy in breast cancer. *J Clin Oncol* 1999;17:1474–81.
- Patino GA, Claes LRF, Lopez-Santiago LF, et al. A functional null mutation of *SCN1B* in a patient with Dravet syndrome. *J Neurosci* 2009;29:10764–78.
- Li Q, Lau A, Morris TJ, et al. A syntaxin 1, $\text{G}\alpha$, and N-type calcium channel complex at a presynaptic nerve terminal: analysis by quantitative immunocolocalization. *J Neurosci* 2004;24:4070–81.
- Conley SJ, Gheordunescu E, Kakarala P, et al. Antiangiogenic agents increase breast cancer stem cells via the generation of tumor hypoxia. *Proc Natl Acad Sci USA* 2012;109:2784–9.
- Jallal H, Valentino ML, Chen G, et al. A Src/Abl kinase inhibitor, SKI-606, blocks breast cancer invasion, growth, and metastasis in vitro and in vivo. *Cancer Res* 2007;67:1580–8.
- Pavlidis P, Noble WS. Matrix2png: a utility for visualizing matrix data. *Bioinformatics* 2003;19:295–6.
- Patino GA, Brackenbury WJ, Bao Y, et al. Voltage-gated Na^+ channel $\beta 1B$: a secreted cell adhesion molecule involved in human epilepsy. *J Neurosci* 2011;31:14577–91.
- Agarwal N, Adhikari AS, Iyer SV, et al. MTBP suppresses cell migration and filopodia formation by inhibiting *ACTN4*. *Oncogene* 2013;32:462–70.
- Philippart U, Roussos ET, Oser M, et al. A Mena invasion isoform potentiates EGF-induced carcinoma cell invasion and metastasis. *Dev Cell* 2008;15:813–28.
- Meyer AS, Hughes-Alford SK, Kay JE, et al. 2D protrusion but not motility predicts growth factor-induced cancer cell migration in 3D collagen. *J Cell Biol* 2012;197:721–9.

38. Maness PF, Schachner M. Neural recognition molecules of the immunoglobulin superfamily: signaling transducers of axon guidance and neuronal migration. *Nat Neurosci* 2007;10:19–26.
39. Yadav V, Denning MF. Fyn is induced by Ras/PI3K/Akt signaling and is required for enhanced invasion/migration. *Mol Carcinog* 2011;50:346–52.
40. Brackenbury WJ, Djamgoz MB. Activity-dependent regulation of voltage-gated Na⁺ channel expression in Mat-LyLu rat prostate cancer cell line. *J Physiol* 2006;573:343–56.
41. Lopez-Santiago LF, Pertin M, Morisod X, et al. Sodium channel beta2 subunits regulate tetrodotoxin-sensitive sodium channels in small dorsal root ganglion neurons and modulate the response to pain. *J Neurosci* 2006;26:7984–94.
42. Kurenova E, Xu LH, Yang X, et al. Focal adhesion kinase suppresses apoptosis by binding to the death domain of receptor-interacting protein. *Mol Cell Biol* 2004;24:4361–71.
43. Li DM, Feng YM. Signaling mechanism of cell adhesion molecules in breast cancer metastasis: potential therapeutic targets. *Breast Cancer Res Treat* 2011;128:7–21.
44. Jansson KH, Lynch JE, Lepori-Bui N, et al. Overexpression of the VSSC-associated CAM, beta-2, enhances LNCaP cell metastasis associated behavior. *Prostate* 2012;72:1080–92.
45. Schafer MK, Altevogt P. LICAM malfunction in the nervous system and human carcinomas. *Cell Mol Life Sci* 2010;67:2425–37.
46. Brisson L, Driffort V, Benoist L, et al. NaV1.5 Na(+) channels allosterically regulate the NHE-1 exchanger and promote the activity of breast cancer cell invadopodia. *J Cell Sci* 2013;126:4835–42.
47. Brisson L, Gillet L, Calaghan S, et al. Na(V)1.5 enhances breast cancer cell invasiveness by increasing NHE1-dependent H(+) efflux in caveolae. *Oncogene* 2011;30:2070–6.
48. Wolf K, Wu YI, Liu Y, et al. Multi-step pericellular proteolysis controls the transition from individual to collective cancer cell invasion. *Nat Cell Biol* 2007;9:893–904.
49. Friedl P, Locker J, Sahai E, Segall JE. Classifying collective cancer cell invasion. *Nat Cell Biol* 2012;14:777–83.
50. Liotta LA, Clair T. Cancer. Checkpoint for invasion. *Nature* 2000;405:287–288.